Processing of rare earth phosphate concentrates: A comparative study of pre-leaching with perchloric, hydrochloric, nitric and phosphoric acids and deportment of minor/major elements

Stone, K.; Bandara, A.M.T.S.; Senanayake, G.; et.al.

Stone, K., Bandara, A. M. T. S., Senanayake, G., & Jayasekera, S. (2016). Processing of rare earth phosphate concentrates: A comparative study of pre-leaching with perchloric, hydrochloric, nitric and phosphoric acids and deportment of minor/major elements. Hydrometallurgy, 163, 137–147. https://doi.org/10.1016/j.hydromet.2016.03.014
Document Version: Author's Version

Published Version: https://doi.org/10.1016/j.hydromet.2016.03.014

Processing of rare earth phosphate concentrates: A comparative study of pre-leaching with perchloric, hydrochloric, nitric and phosphoric acids and deportment of minor/major elements

K. Stone[a], A.M.T.S. Bandara[a], G. Senanayake[a*] and S. Jayasekera[a,b]

[a]Chemical and Metallurgical Engineering and Chemistry, School of Engineering & Information Technology, Murdoch University, 90 South Street, Murdoch, Perth, WA 6150 Australia
[b]SJ Mets Consulting Pty Ltd, PO Box 1509 Booragoon, WA 6954 Australia

ABSTRACT

Phosphate rocks such as fluorapatite often contain significant amounts of rare earth minerals and considered as rare earth ores. They can be processed to produce phosphoric acid as well as rare earth metals. The mineralization, however, is commonly associated with other rare earth minerals such as monazite ($(Ce,La,Th,Nd,Y)PO_4$), florencite ($(La,Ce)Al_3(PO_4)_2(OH)_6$), xenotime ($YPO_4$) and cheralite ($(Ca,Ce)(Th,Ce)(PO_4)_2$). The treatment of fluorapatite for rare earth extraction commonly requires a pre-leach stage with a mineral acid. Calcium, sodium, magnesium, aluminum, potassium, iron, manganese. A range of other metals such as uranium and thorium may enter the solution depending upon the oxide/phosphate/silicate mineralogy. Further processing may involve partial neutralisation to precipitate any rare earth metals which may have solubilised during pre-leach, acid bake of the residue/precipitate with sulphuric acid, water leach followed by purification and precipitation. This paper describes results from a comparative study conducted on pre-leaching a phosphate rare earth concentrate using perchloric, hydrochloric, nitric and phosphoric acids under various leach conditions including different acid concentrations, temperatures and solid/liquid ratios. Through equilibrium constants and kinetic data including measured leachability of relevant metal ions, the study suggests an alternative process route which involves a selective phosphoric acid pre-leach causing low deportment of rare earth elements, uranium and thorium leading to a potentially more efficient downstream process.

Key Words

Rare earth, acid leaching, phosphate, fluorapatite, uranium, thorium

*Tel.: +61 8 93602833; fax: +61 8 93606343.
E-mail address: G.Senanayake@murdoch.edu.au

1. INTRODUCTION

The rare earth elements (REEs) are a unique group of metals regarded as being among the most critical elements that are highly valued for their specialised application in many modern technologies. In recent years, REEs have become a significant topic of interest in the metals industry due to a global supply shortage and strengthening demand (Investor Intel, 2015; European Union, 2014). This has led many companies to develop processing techniques for extracting REEs from less common rare earth bearing deposits (Jorjani *et al.*, 2011) and reclaiming REEs from end-of-life products by recycling (urban mining) spent batteries, phosphors and permanent magnets (Tunsu et al., 2015). One such example is the apatite group of minerals (mainly fluorapatite) which are commonly mined for the production of phosphoric acid in the fertiliser industry (Olanipekun, 1999; Dippel, 2004). Apatite ores are known to contain significant quantities of REEs and therefore processing of apatite ores for REEs has become more prominent recently (Wang *et al.*, 2010). These deposits however, often require a pre-leach stage prior to the acid bake stage at elevated temperature where the latter converts REE-phosphates to water soluble REE-sulphates (Gupta and Krisnamurthy, 2005). Some of the reactions involved in the pre-leach stage are listed in Table 1. The aim of the pre-leach stage of ores/concentrates is to remove the calcium which otherwise interfere with liberation of REEs in acid bake stage due to formation of gypsum. However, the results from prior test work on the pre-leaching of some concentrates using hydrochloric and nitric acid showed that significant amount of REEs were also solubilised in the process which is undesired (Beer *et al.*, 2008).

Any rare earth metal ions leached with hydrochloric acid can be precipitated by the addition of limestone to produce a pre-leach residue and precipitate, rich in phosphate and REEs. The pre-leach liquor could then be passed onto a number of stage-wise precipitation processes where limestone and lime are added to recover the uranium, fluoride, gypsum ($CaSO_4.2H_2O$) and di-calcium phosphate ($CaHPO_4.2H_2O$) (Senanayake et al., 2014b). Through the addition of sulphuric acid, hydrochloric acid can be regenerated and recycled back to the pre-leach process (Feldmann and Demopoulos, 2015). On the other hand, if phosphoric acid is used for the pre-leach (Eq. 4a), by the addition of H_2SO_4 to pre-leach liquor (Eq.4c), phosphoric acid can be regenerated and recycled to leach. Excess phosphoric acid regenerated can be a saleable by-product which may enhance the economic viability of a process.

For this reason, a better understanding of solubilities of rare earth metal ions and controlling the deportment of elements such as uranium, thorium, iron and aluminium are particularly important. Recent studies have focussed on a systematic study on (i) the solubility of rare earth metal ions in different acids and liquors of compositions similar to those of process liquors, (ii) leachability of metal ions from fluoroapatite as well as from a rare-earth phosphate concentrate and (iii) the treatment of the pre-leach liquor to precipitate calcium phosphate as a saleable product (Senanayake et al., 2014a, b; Bandara and Senanayake, 2015).

This work aims to briefly review the previous studies and compare the leaching of fluorapatite in different acids (perchloric, hydrochloric, nitric and phosphoric acids) at comparable conditions using two natural fluorapatite samples and a rare earth bearing fluorapatite concentrate. The reason for using perchloric acid for comparison was to specifically compare the effect of anions. The study also aims to investigate the effect of phosphoric acid concentration, temperature and pulp density on the leaching of fluorapatite and the concentrate.

2. PREVIOUS STUDIES

Arguably the most common use of apatite is in the production of fertilisers and phosphoric acid due to the high content of phosphorus (Olanipekun, 1999). In this process, sulphuric acid is used to produce phosphor-gypsum, phosphoric acid and hydrofluoric acid according to reaction 1 in Table 1. Hydrochloric acid and nitric acid have been used in many apatite leaching studies (Zafar *et al.*, 2006; Dorozhkin, 2012; Habashi, 1998) and have shown high calcium and phosphate leaching. In all cases REEs are leached and therefore a re-precipitation is required before the acid bake process. Sulphuric acid is not favoured in pre-leach due to potential entrainment of REEs, in the phosphor-gypsum precipitate.

The solubility of rare earth phosphates in phosphoric acid, which is also produced in reactions 2 and 3 in Table 1 as well as with perchloric acid, is low due to the common ion effect, i.e. phosphate ions in both the solid and solution phases (Migddisov *et al*., 2009; Cetiner et al., 2005; Liu and Byrne, 1997). For this reason, prior studies into the leaching of REEs present in apatite ores using phosphoric acid are limited. However, the results from fluorapatite leaching with phosphoric acid show high solubility of calcium and phosphate which in turn suggest the

potential application of phosphoric acid in the pre-leaching stage. (Brahim *et al.*, 2008; Antar and Jemal, 2008).

Test work into the acid pre-leach stage of a rare earth phosphate concentrate using nitric acid and hydrochloric acid has been conducted previously by Mackowski *et al.* (2011). It was found that the nitric acid pre-leaching study was effective in dissolving 97% and 94% of the calcium and phosphorus, respectively, whilst the extraction of the light REEs (La, Ce, Pr and Nd) was 40%. The pre-leach with hydrochloric acid showed similar results, but the dissolution of key REEs present (La, Ce and Nd) was approximately 10% lower. Figure 1 shows the comparison of the HNO_3 and HCl pre-leach study results of the same concentrate based on the conditions listed in Table 2. It must be noted that the plot in Figure 1 is purely for comparison purposes only and it must not be interpreted as one study being dependent on the other. Interestingly, the plot shows that calcium, phosphorus, fluoride and silicon gave comparable leaching efficiencies (%) in the two acids, as the data points lie on the straight line of slope 1 through the origin. However, nitric acid was more effective in solubilising the REEs than hydrochloric acid, as the data points for REEs lie below the line of slope 1.

Figure 2 summarises the results from solubility studies (Senanayake et al., 2014b) and show the precipitation of various metal ions from HCl pre-leach liquors which contained: Ca (90 g/L), Al (8 g/L), Fe (5.8 g/L), F (4.4 g/L), K (3.6 g/L), Mg (1.2 g/L), Na (0.3 g/L), P (29 g/L), S (0.16 g/L) , Th (6.6 mg/L) and U (66 mg/L). The solubility of calcium salts of interest to this study in pure water (shown in brackets in mmol/L at 20-25^{o}C) follows the descending order: $Ca(H_2PO_4)_2$ (77) > $CaSiF_6$ (28.4) > $Ca(OH)_2$ (23) > $CaHPO_4$ (0.3) > CaF_2 (0.2) > $CaCO_3$ (0.07) > $Ca_3(PO_4)_2$ (0.06) (http://en.wikipedia.org/wiki/Solubility_table). Thus, the neutralisation of acid in the pre-leach liquor with the addition of limestone caused the precipitation of calcium in the form of dicalcium phosphate (DCP, $CaHPO_4$) and monocalcium phosphate (MCP, $Ca(H_2PO_4)_2.2H_2O$). The increase in slurry pH also caused the precipitation of other ions as shown in Figure 2. Thus, calcium phosphate can be effectively separated from fluoride, uranium and thorium using a two stage selective precipitation with calcium carbonate at pH 0.3 (stage 1) and pH 3 (stage 2) (Senanayake et al., 2014b).

The lack of comparability of conditions in Table 2 highlights the need for a proper comparative/systematic study of the pre-leach stage with different acids. The results from previous work highlight (i) the potential scope for further investigation into optimising the leach conditions in controlled systems, (ii) the importance of comparing leach results with different

lixiviants such as perchloric, nitric, hydrochloric and phosphoric acid, and (iii) investigating the leaching behaviour of fluorapatite alone (i.e. without the presence of other minerals) to rationalise the leach chemistry (Bandara and Senanayake, 2015). The objectives of the present study are listed below:

- Investigate the leachability of fluorapatite and a phosphate concentrate using perchloric, hydrochloric, nitric and phosphoric acids under comparable conditions (i.e. controlled temperature, acid concentration, pulp density, agitation rate and leach duration).
- Investigate the use of phosphoric acid as a potential lixiviant for leaching fluorapatite by examining the effect of changing acid concentration, pulp density, operating temperature and leach duration.
- Examine the deportment of rare earth elements, as well as other key elements such as uranium, thorium, iron and aluminium in both leach liquor and solid residue.
- Explain the trends using equilibria related to solubility and complex formation.

3. EXPERIMENTAL

The particle size distribution (PSD) for the concentrate was determined using a Microtrac S3500 laser sizing machine. After obtaining the 80% passing size (P_{80}) of the concentrate from the PSD, the large crystals of fluorapatite (as received) were crushed using a pulverising ring mill to produce a similar P_{80}. The head assays were performed by TSW Analytical Pty Ltd. (Perth, Western Australia) and Murdoch University Laboratories using Inductive Coupled Plasma Atomic Emission Spectroscopy (ICP-AES) and Mass Spectroscopy (ICP-MS). The XRD scans were performed using the X-ray diffractometer (GBC Enhanced Minimaterial Analyser (EMMA), Theta-Theta Diffractometer). Scans were completed for an angle range of 10° to 90^{o} and the results were compared to the characteristic peaks from the database of International Centre for Diffraction Data (ICDD).

High purity millipore water was used throughout all experiments, to reduce the potential for contaminants affecting the results of the leach studies. All acids used in the experiments were analytical grade. The reactor used in all leaching experiments contained three baffles evenly spaced around the inside of the vessel. The lid of the vessel housed the overhead agitator (3 blades) and drive motor. A digital tachometer was used to measure rotation speed of the agitator maintained at 1100 rpm to ensure the solids were adequately suspended in the fluid. The experimental details on leaching have been reported in previous publications (Senanayake et al., 2010). Once the solids were added, the leaching timer was started and the temperature of the system was monitored using a thermometer. The slurry samples were taken at set time intervals (0, 10, 20, 30 min and 1, 2, 4 h) from the reactor using a 50 mL syringe attached to a 20 cm length of tube. The slurry was immediately filtered using a Buchner vacuum filtration system. The filtrate was poured into 30 mL sample jars, while the filter paper and solid contents were taken for further drying. Once the samples were dry, the weight of the solid residue was taken. A summary of the experimental program is shown in Table 3. The test parameter boundaries were determined by previously published studies. Acid concentration was determined by the pulp density of the slurry and the mass of solid required using the stoichiometry shown in Table 1 and the requirements as shown in Table 3.

4. RESULTS AND DISCUSSION

4.1 Characterisation

4.1.1 Feed materials

Figures 3 and 4 show the results of the XRD scans for fluorapatite and the phosphate concentrate. The matching with characteristic peaks confirms the purity of the FAP samples (Figure 3) and the presence of fluorapatite, cheralite, calcium silicate and monazite (Figure 4) in the phosphate concentrate. The 80% passing size (P_{80}) was 165 µm and 205 µm, respectively, for the concentrate and fluorapatite based on laser sizing. The head assays of the concentrate and fluorapatite samples are presented as non-REEs (Table 4) and REEs (Table 5) for easy comparison. The REEs are present in varying compositions, with the light rare earth elements of lanthanum, cerium and neodymium being the most prominent in the concentrate. The total REEs (lanthanides + yttrium) contents are 4.91%, 1.25% and 0.55% in concentrate, FAP1 and FAP2, respectively. Figure 5 plots the composition of REEs in FAP1 and FAP2 as a function of that in concentrate to show that there is a reasonably linear correlation highlighting that the leaching studies based on natural FAP samples are useful for the rationalisation of leaching behaviour of metals from the phosphate concentrate.

4.1.2 Leach residues of phosphate concentrate

The assays of the leach residues of the phosphate concentrate obtained in different acids are listed in Table 6. The results indicate higher residual REEs in leach residues produced from all solutions of H_3PO_4 (6.47% - 9.65%) compared to lower values in HCl and HNO_3 (2.77% - 4.18%). The highest and lowest enrichment of total REEs in H_3PO_4 are caused by the pre-leach in 3.25 mol L^{-1} (9.65%) and 2.28 mol L^{-1} (6.47%) solutions, respectively, at 95 ^{o}C. Moreover, low contents of Al, Fe and Si and high contents of Th in leach residues generated using H_3PO_4 at 95 ^{o}C, compared to other acids, may be the potential advantages of using phosphoric acid as the lixiviant during pre-leach of REE-fluorapatite concentrates.

4.2 Leaching of fluroapatite

The leach duration for tests FAP1 and FAP2 using H_3PO_4 was 4 hours. However, the tests using HCl and HNO_3 were concluded at 30 minutes and 2 hours, respectively, due to 100% dissolution of the initial fluorapatite solid. These observations are reflected in the results summarised in Table 7 and Figure 6, which shows that high dissolution of calcium in the HCl and HNO_3 was achieved within the first 20 minutes. Table 8 lists the equilibrium constants for the dissociation of H_3PO_4 to various ions (H^+, $H_2PO_4^-$, HPO_4^{2-}, PO_4^{3-}) and the formation constants of the various ion-pairs of phosphate complex species of calcium, iron and aluminium ions (e.g. $CaH_2PO_4^+$, $CaHPO_4^0$). Despite the high stability of the calcium ions in solution in the form of complex species, the tests with H_3PO_4 shows a slower leaching rate of FAP and approximately 73% dissolution after 4 hours (Figure 6). This behaviour can be rationalised on the basis of lower proton activity (higher pH) of H_3PO_4 compared to other acids at a given concentration (Bandara and Senanayake, 2015). Table 9 summarises the Ca/P ratio results based on the fluorapatite formula, stoichiometry (theoretical ratio) and the final leach liquor results from each acid. The purpose of analysing the Ca/P ratio is to investigate whether the H_3PO_4 leach system has produced a surface blocking species which retards the leaching of calcium as shown in Figure 6. As the results in Table 9 show, the Ca/P molar ratios in $HClO_4$, HCl and HNO_3 closely agree with the theoretical ratio of 1.7 in the fluorapatite. The H_3PO_4 test however, showed a significantly lower molar ratio of Ca/P = 0.6 compared to the ratios based on assays and tests with other acids. Similar studies based on the second sample of FAP (FAP2 in Table 4) showed shrinking core kinetics indicating that the FAP surface is changing from the normal FAP structure to a calcium rich product layer (Bandara and Senanayake, 2015). Nevertheless, Figure 7 shows reasonably good linear correlation of slope 1 for the plot of composition of Ca, P, F, Mg, Fe and Al (mg/L) in leach liquors produced from HCl, HNO_3 and H_3PO_4 as a function of that of $HClO_4$. This indicates the fact that the different anions from acids have no significant influence on the leaching of FAP, as described by the reactions in Table 1, except for the kinetic effects reported previously (Bandara and Senanayake, 2015).

4.3 Leaching of concentrate

A summary of the results from the leaching experiments of the concentrate using $HClO_4$, HCl, HNO_3 and H_3PO_4 at different acid concentrations, solid/liquid ratios and temperatures are shown in Table 10 and Figures 8-11. A brief discussion on the effect of different acids and conditions is presented below.

4.3.1 Effect of different acids

(a) Leaching efficiency

Figures 8a-b show a comparison of the leaching efficiencies of various elements in H_3PO_4 as a function of the leaching efficiencies in HNO_3 (Figure 8a) and HCl (Figure 8b). As the plots depict, majority of the elements (except magnesium) showed higher leaching efficiency in HCl and HNO_3 compared to that in H_3PO_4. Uranium, thorium and the rare earth elements showed particularly low leaching efficiencies in H_3PO_4 compared to those in HNO_3 and HCl, as shown in the cluster of elements in bottom right corner of both plots. These results will be explained in further detail in subsequent discussions. The leach curves for calcium, uranium, aluminium and iron with each of the different acids are shown in Figure 9a–d. These plots indicate several features such as: (i) the relatively fast leach kinetics shown by some systems reaching 100% leaching efficiency in a short time (Figure 9a), (ii) slow continuous leaching (Figure 9c-d) and (iii) the formation of precipitates during prolonged leaching (Figure 9b).

As shown in Figure 9a, 100% of the calcium present in the concentrate was leached in HCl and HNO_3, but only 85% leaching was observed in H_3PO_4. As shown in Table 9, the Ca/P molar ratio calculated for the concentrate based on the initial solid head assay is 2.4. This may be compared to the experimental Ca/P molar ratio determined from the final 4 hour leach liquor assays which vary in the descending order: HCl (2.7) > HNO_3 (2.3) > H_3PO_4 (1.7) . The lower experimental molar leaching ratio of Ca/P in H_3PO_4 is consistent for both concentrate and FAP as shown in Table 9. The leaching efficiency of fluoride from the concentrate in H_3PO_4 is close to 30% (Table 10) compared to 100% in the case of FAP (Bandara and Senanayake, 2015), which can be related to the presence of other minerals associated with the concentrate noted in Figure 4. Nevertheless, the leach curve for calcium shown in Figure 9(a) for concentrate and that in Figure 6 for FAP1 follow similar trends indicating that leach products may be forming on

the surface of both FAP and concentrate particles during leaching, resulting in lower leach efficiency of calcium compared to phosphorous (phosphate). The leaching efficiency of rare earth elements in the three acids, HCl, HNO_3 and $HClO_4$ was considerably higher compared to that in H_3PO_4 due to the fact that REEs were present in the concentrate as rare earth phosphates as replacements in the crystal lattice for calcium (Fleet and Pan, 1995).

(b) Chemical species and equilibrium constants

Table 11 lists the equilibrium constants for the formation of rare earth phosphate complexes in solution as well as the rare earth phosphate solid (MPO_4). The data show that rare earth phosphates are more stable as solids, as indicated by large equilibrium constants, than as complex species in solution. This indicates that rare earth phosphate leaching was expected to be low in H_3PO_4. The formation of both HF and H_3PO_4 during leaching in all cases (Table 1) highlights the importance of considering the equilibrium constants related to the formation of fluoride complexes as well as the formation and dissolution of phosphate precipitates with various metal ions present in the system, listed in Tables 12 and 13. The high formation constant of the uranium phosphate precipitates listed in Table 13 (Reaction 50-52) rationalises the low leaching efficiency of uranium in H_3PO_4. The tables also show that the formation constant for HF and HF_2^- and fluoride complexes of calcium and magnesium ions (Reaction 20-23) are low relative to the data for metal ion complexes of aluminium and iron (Reaction 24-32), explaining the higher extent of leaching of aluminium and iron (Table 10). The differences in leaching behaviour of aluminium in HCl and H_3PO_4 can also be explained on the basis of the formation of complexes. Comparison of reactions 44, 46 and 47 in Table 13 show the possibility of dissolution of aluminium as AlF_4^- due to the large equilibrium constant for reaction 47. The formation of the highly stable AlF_4^- complex ion facilitates the high leaching efficiency of aluminium in HCl and HNO_3 in Table 10. However, in the case of H_3PO_4, $H_2PO_4^-$ is the predominant anion (see reaction 4b in Table 1). This favours the reverse of reaction 47 and the formation of the aluminium phosphate precipitate leading to lower leaching efficiency of aluminium in H_3PO_4 in Table 10.

4.3.2 Effect of H_3PO_4 concentration

The results in Table 10 show that the leaching efficiencies of calcium, iron and aluminium increase with the increase in acid concentration. The increase in calcium leaching can be accompanied by the formation of HF in solution (reactions 4 a,b in Table 1), which enhances leaching of aluminium and iron due to the formation of stable complex ions in solution (reactions 47 and 49 in Table 13). However, uranium and thorium showed decreasing leaching efficiencies with increasing acid concentration. The leach curve for uranium at different acid concentrations is shown in Figure 10a. The plot indicates that the formation of a precipitate occurred after 10 minutes of leaching in acid at higher concentrations. This may be attributed to the precipitation of uranium as $Ca(UO_2)_2(PO_4)_2.3H_2O$ according to reaction 50 in Table 13. Thus, increased leaching of calcium at higher concentrations of H_3PO_4 is detrimental to the leaching of uranium. The influence of phosphoric acid concentration on the leaching of rare earth metal ions is not as profound as the difference observed in different acids (Table 10). The low leaching of REEs in H_3PO_4 is largely a result of the phosphate precipitation discussed previously and is confirmed in the leach curve of lanthanum shown in Figure 10b. The different leaching behaviour of elements in H_3PO_4 solutions of different concentrations is also depicted in Figures 10c-d. Although the leaching efficiency of calcium, iron, manganese and aluminium increases with the increase in concentration of H_3PO_4, uranium, thorium and REEs show much lower values (corresponding to <10 mg/L) at higher acid concentrations. Further investigation into the uranium and rare earth speciation is required for better understanding.

4.3.3 Effect of temperature and pulp density

Table 10 shows that the leaching efficiency of calcium decreased from 99% to 85% with increasing temperature. Likewise, as shown in Figure 11, the leaching efficiency of uranium decreased with increasing temperature, whilst at 95 °C uranium formed a precipitate. Further investigation is required to confirm the formation of these precipitates. In terms of rare earth leaching, the log K values in Table 14 show that a small decrease in solubility is expected. Thus, a systematic study is essential to understand the solubility behaviour of rare earth phosphates at the desired temperatures.

A summary of the results from the experiments at different pulp densities is shown in Table 10. It was expected that as the pulp density of the system decreased, the leaching efficiency of the elements in the concentrate would increase due to enhanced lixiviant and

particle interaction giving greater contact time. However, this prediction was not reflected in the leach results as the 10% solids (w/w) appear to be the most effective in leaching calcium, iron and aluminium. Further test work would be required in this area.

4.3.4 Comparison of pre-leach options

As noted in sections 1 and 2 (Figure 1) , the pre-leach of phosphate concentrates using hydrochloric acid dissolves all calcium and a significant amount of REEs (Beer *et al.*, 2008). Limestone and lime are added to the leach liquor to recover the uranium, fluoride, gypsum and di-calcium phosphate (Senanayake et al., 2014b), while the hydrochloric acid regenerated with sulphuric acid can be recycled back to the pre-leach process (Feldmann and Demopoulos, 2015). In contrast, the maximum leaching efficiencies of calcium (100%) keeping dissolution of REEs at a minimum level in H_3PO_4 at high acid concentrations (Tables 10 and 14) shows a positive impact on selecting H_3PO_4 as a pre-leaching agent, instead of HCl. Moreover, Table 1 shows that the leaching of a mole of $Ca_5(PO_4)_3F$ requires 7 moles of H_3PO_4 (equation 4a) whereas the regeneration of acid with H_2SO_4 produces 10 moles of H_3PO_4 (equation 4c), leading to the overall pre-leach reaction in equation 1, which is the same as pre-leach with H_2SO_4. Unlike sulphuric acid which is not favoured in direct pre-leach due to potential entrainment of REEs, in the phosphor-gypsum precipitate, the phosphoric acid pre-leach offers two advantages: (i) the production of a rare earth enriched residue which can be further processed using standard methods described in the literature (Gupta and Krisnamurthy, 2005), (ii) the regenerated H_3PO_4 can be recycled for pre-leach and the excess can be further treated for fertiliser production. According to the data presented in Tables 6 and 10, the most suitable leaching conditions to minimise the deportment of REEs, uranium and thorium appears to be 3.25 mol/L H_3PO_4, 5% (w/w) solids at 95 ^oC over 4 h. Although a simplified conceptual block diagram is shown in Figure 12, further work with continuous leaching and recycling is essential to rationalise the build up of impurities and the viability of the flowsheet.

5. CONCLUSIONS

A comparative study on the acid pre-leach of fluorapatite and a rare earth phosphate concentrate was conducted to investigate the leachability of the fluorapatite component using $HClO_4$, HCl, HNO_3 and H_3PO_4, to determine the most effective acid. The results showed high leaching of calcium and phosphate in $HClO_4$, HCl and HNO_3, but low leaching in H_3PO_4. Rapid and increased leaching efficiencies of calcium, phosphate and fluoride as well as other metal ions are consistent with the formation of phosphate/fluoride complex species in solution evident from published equilibrium constants. The REEs present in the concentrate showed considerably higher leaching efficiency with $HClO_4$, HCl and HNO_3, compared to that with H_3PO_4 due to the formation of rare earth phosphate precipitates. The lower aluminium and iron leaching in H_3PO_4 indicated the opposing effects of fluoride complexation and phosphate precipitation. The leaching efficiency of calcium, iron, manganese and aluminium increased with increasing acid concentration due to the formation of fluoride/phosphate complexes. Uranium showed lower leaching efficiency with increasing acid concentration due to the formation of uranyl phosphate precipitates demonstrated by the leach curves. The test results at different temperatures showed that uranium formed a precipitate at higher temperatures. However, the pulp density was less influential on leaching compared to acid type and acid concentration. In summary, the results have shown that phosphoric acid could be a suitable lixiviant in the pre-leaching process for rare earth bearing fluroapatite concentrates for selective leaching of calcium and some other metals leaving uranium, thorium and REEs in the residue suitable for acid bake.

REFERENCES

Antar, K., Jemal, M., 2008. Kinetics and thermodynamics of the attack of a phosphate ore by acid solutions at different temperatures. Thermochimica Acta. 474, 32-35.

Bandara, A.M.T.S., Senanayake, G., 2015. Leachability of rare-earth, calcium and minor metal ions from natural Fluorapatite in perchloric, hydrochloric, nitric and phosphoric acid solutions: Effect of proton activity and anion participation. Hydrometallurgy 153, 179-189.

Beer, G., Mackowski, S., Raiter, R. (on behalf of Arafura Res.), 2008. Development of a Processing Flowsheet for the Nolans Project. Proceedings of ALTA Uranium 2008, ALTA Metallurgical Services, Perth (WA), 1-30.

Brahim, K., Antar, K., Khattech, I., Jernal, M., 2008. Effect of temperature on the attack of fluorapatite by a phosphoric acid solution. 2, 35- 39

Cetiner, Z., Wood, S., Gammons, C., 2005. The aqueous geochemistry of the rare earth elements. Part XIV. The solubility of rare earth element phosphates from 23 to 150°C. Chemical Geology. 217, 147-169.

Dippel, S.K., 2004. Mineralogical and Geochemical Characterisation of Phosphogypsum Waste Material and its Potential for use as backfill at WMC Fertilizers' Mine Site, Phosphate Hill, N-W Queensland, Thesis, James Cook University: Townsville, QLD. http://eprints.jcu.edu.au/103/ (Accessed: Feb 27, 2012).

European Union, 2014. Report on Critical Raw Materials for EU. http://ec.europa.eu/enterprise/policies/raw-materials/files/docs/crm-report-on-critical-raw-materials_en.pdf

Feldmann, D., Demopoulos, G.P., 2015. Water activity-based design of a single-stage CSTR reactive crystallization process for producing super-azeotropic HCl and well grown metastable α-calcium sulfate hemihydrate crystals from $CaCl_2$ solution. Hydrometallurgy 155, 20-28.

Dorozhkin, S., 2012. Dissolution mechanism of calcium apatites in acids: A review of literature. World of Methodology. 26, 1-17.

Firsching, F.H., Brune, S.N., 1991. Solubility products of the trivalent rare-earth phosphates. J. Chem. Eng. Data 36, 93– 95.

Fleet, M., Pan, Y., 1995. Site preference of rare earth elements in fluorapatite. American Metallurgist. 80, 329- 335.

Gorman-Lewis, D., Shvareva,T., Kubatko, K., Burns, P., Wellman, D., McNamara, B., Szymanowski, J., Navrotzky, A., Fein, J., 2009. Thermodynamic Properties of Autunite, Uranyl Hydrogen Phosphate, and Uranyl Orthophosphate from Solubility and Calorimetric Measurements. Enviro. Sci. Technol. 43, 7416- 7422.

Gupta, C.K., Krishnamurthy, N., 2005. Extractive Metallurgy of Rare Earths, first edition.CRC Press, Boca Raton, Florida.

Habashi, F., 1998. Solvent extraction in the phosphate fertilizer industry. In *Extraction & Processing Division* 1998 edited by B. Mishra, TMS-AIME, Warrendale, PA. 201-218.

Haynes, W.M., Lide, D.R., Bruno, T.J., 2014-2015. CRC Handbook of chemistry and physics, 95th edition.Hem, J.D., 1968. Graphical methods for studies of aqueous aluminium hydroxide, fluoride and sulphate complexes: chemistry of aluminium in natural water. Geological survey water-supply paper, 1827-B.

Högfeldt, E., 1982. Stability constants of Metal-Ion complexes; Part A – Inorganic ligands. IUPAC chemical data series, No.21

Investor Intel, 2015. http://investorintel.com/technology-metals-video/

Jorjani, E., Bagherieh, A., Chelgani, S., 2011. Rare earth elements leaching from Chadormalu apatite concentrate: Laboratory studies and regression predictions. Korean J. Chem. Eng. 28, 557- 562.

Li, H., Guo, F., Zhang, Z., Li, D., Wang, Z., 2006. A new hydrometallurgical process for extracting rare earths from apatite ores using solvent extraction with P_{350}. Journal of Alloys and Compounds. 408, 995-998.

Liu, X., Byrne, R., 1997. Rare Earth and yttrium phosphate solubilities in aqueous solution. Geochimica et Comoschimica Acta. 61, 1625-1633.

Mackowski, S., Raiter, R., Soldenhoff, K., Ho, E. (on behalf of Arafura Res.), 2011. *Patent*: Recovery of rare earths elements, (Patent No.: US 7,993,612 B2).

Migdisov, A., William-Jones, A., Wagner, T., 2009. An experimental study of the solubility and speciation of the Rare Earth Elements (III) in fluoride- and chloride-bearing aqueous solutions at temperatures up to 300 ◦C. Elsevier. 17, 7087- 7109.

Olanipekun, E., 1999. Kinetics of Dissolution of Phosphorite in Acid Mixtures. Bull. Chem. Soc Ethiop. 13, 63- 70.

Savenko, A.V., Baturin, G.N., Golubev, S.V., 2005. Crandallite solubility in aqueous solutions. Geochem. Int. 43(11), 1135-1137.

Sedlak, R.I., 1991. Phosphorus and nitrogen removal from municipal wastewater, 2nd ed. CRC press , 97-100.

Senanayake, G. Senaputra, A. Nicol, M. J., 2010. Effect of thiosulfate, sulfide, copper(II), cobalt(II)/(III) and iron oxides on the ammoniacal carbonate leaching of nickel and ferronickel in the Caron process. Hydrometallurgy 105, 60-68.

Senanayake, G., Jayasekera, S., Bandara, A. M. T. S., Koenigsberger, E., Koenigsberger, L., Kyle, J., 2014. Rare earth metal ion solubility in acidic sulphate-phosphate solutions. Proceedings of The 7th International Symposium - Hydrometallurgy 2014, Ed: E. Asselin, D. Dixon, F. Doyle, D. Dreisinger, M. Jeffrey, M. Moats, Canadian Institute of Mining, Metallurgy and Petroleum, Victoria, BC, Canada, Vol 1, pp. 313-324.

Senanayake, G., Kyle, J., Hunt, S., Stone, K., Perera, N., Jayasekera, S., 2014. Precipitation of calcium phosphate from hydrochloric acid leach liquor of a rare earth concentrate. Proceedings of The 7th International Symposium - Hydrometallurgy 2014, Ed: E. Asselin, D. Dixon, F. Doyle, D. Dreisinger, M. Jeffrey, M. Moats, Canadian Institute of Mining, Metallurgy and Petroleum, Victoria, BC, Canada, Vol 1, pp. 325-337.

Tunsu, C., Petranikova, M., Gergoric, M., Ekberg, C., Retegan, T., 2015. Reclaiming rare earth elements from end-of-life products: A review of the perspectives for urban mining using hydrometallurgical unit operations. Hydrometallurgy. 156, 239-258.

Wang, L. Long, Z., Huang, X., Yu, Y., Cui, D., Zhang, G., 2010. Recovery of rare earths from wet-process phosphoric acid. Hydrometallurgy. 101, 41- 47.

Wilemon, G., Scheiner, B., 1987. Leaching of Phosphate Values from Two Central Florida Ores Using H_2SO_4 Methanol Mixtures. Int. Bu of Mines. 28496, 1-8.

Zafar, Z.I., Tariq Mahmood, A., Mohammad, A., Mohammad Amin, A., 2006. Effect of Hydrochloric Acid on Leaching Behavior of Calcareous Phosphorites. Iran J. Chem. Chem Eng. 25, 47- 57.

Zhang, F., Yeh, G-T., Parker, J.C., 2012. Groundwater reactive transport models. Bentham science publishers

Ziya, S.C., Scott, A.W., Christopher, H.G., 2005. The aqueous geochemistry of the rare earth elements: Part XIV: The solubility of rare earth element phosphates from 23 to 150 ^{0}C. Chemical Geology 217, 147– 169.

Figure 1

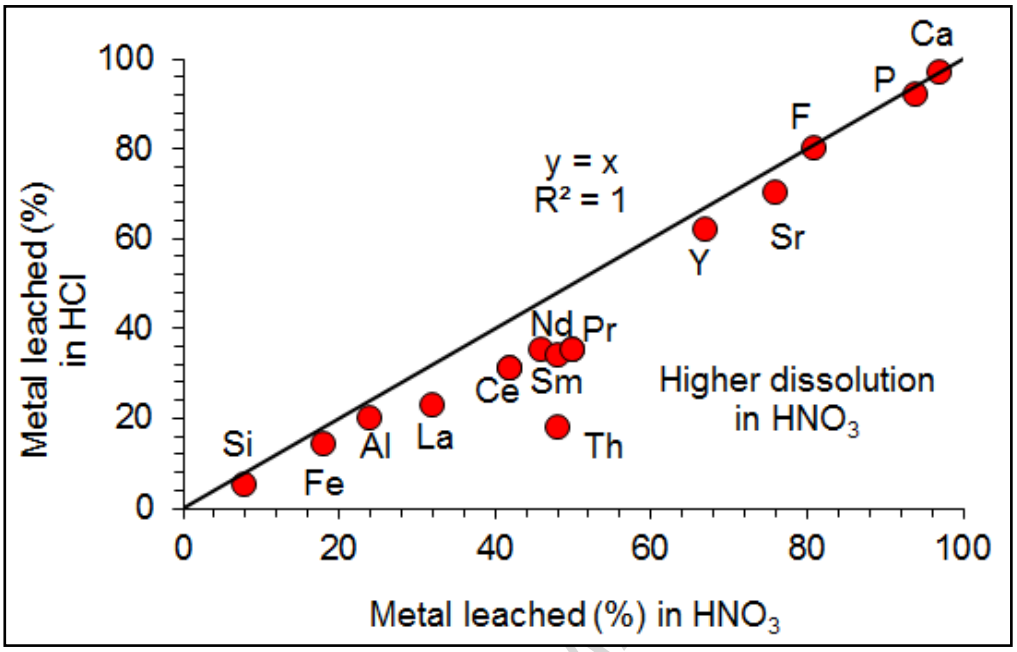

Figure 1. Pre-leach results with hydrochloric and nitric acids (Mckowski et al., 2011; see Table 2 for leach conditions)

Figure 2

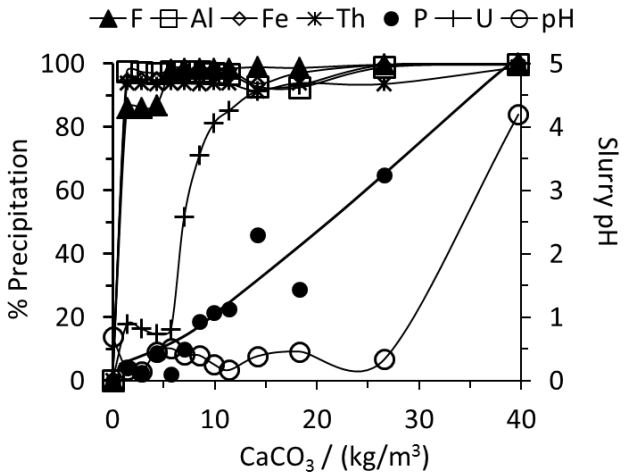

Figure 2. Precipitation of metal ions from hydrochloric acid pre-leach liquor with the addition of limestone/lime (data from Senanayake et al., 2014b).

Figure 3

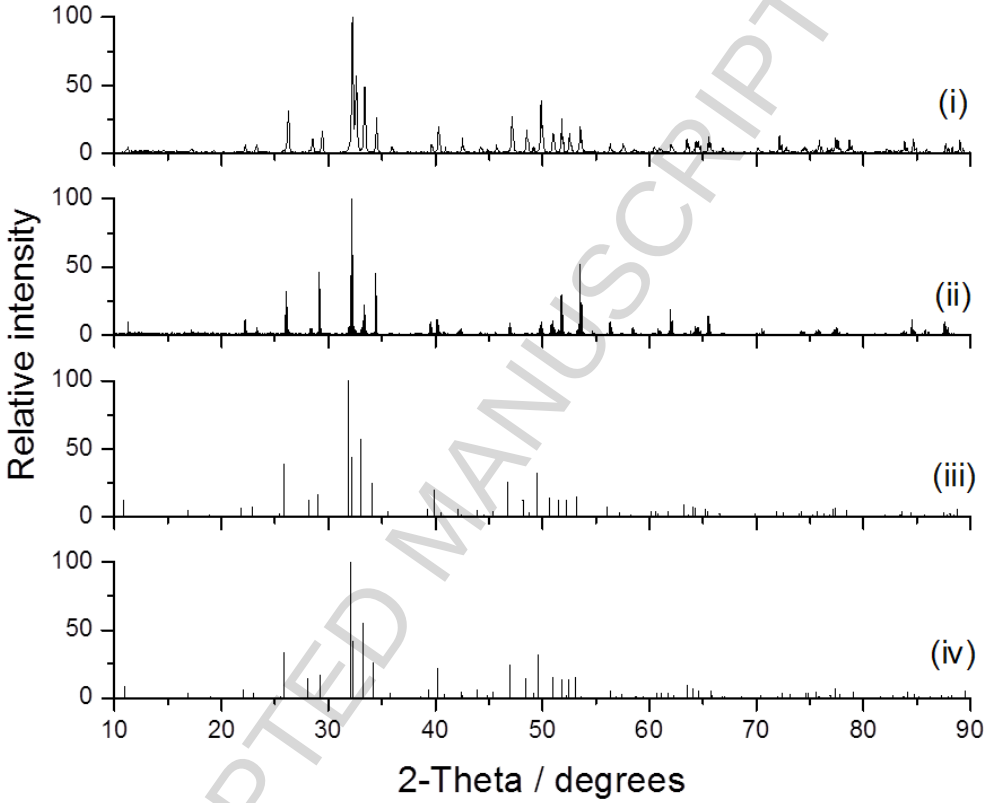

Figure 3. XRD patterns of FAP samples (i) FAP-1 and (ii) FAP-2; Comparison with standard patterns: (iii) FAP (01-071-5050) and (iv) carbonate-FAP (01-073-9696)

Figure 4

(a)

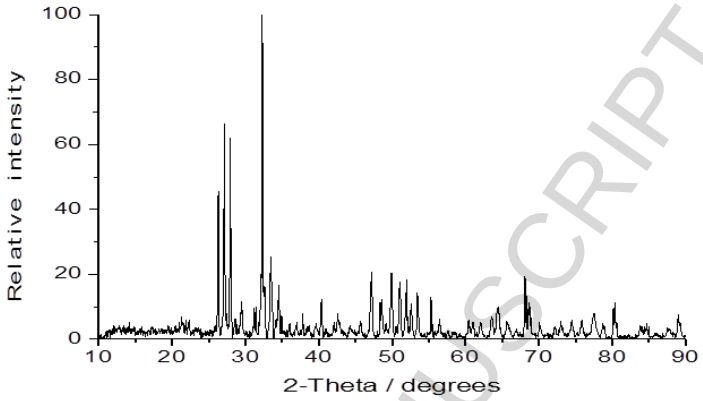

(b)

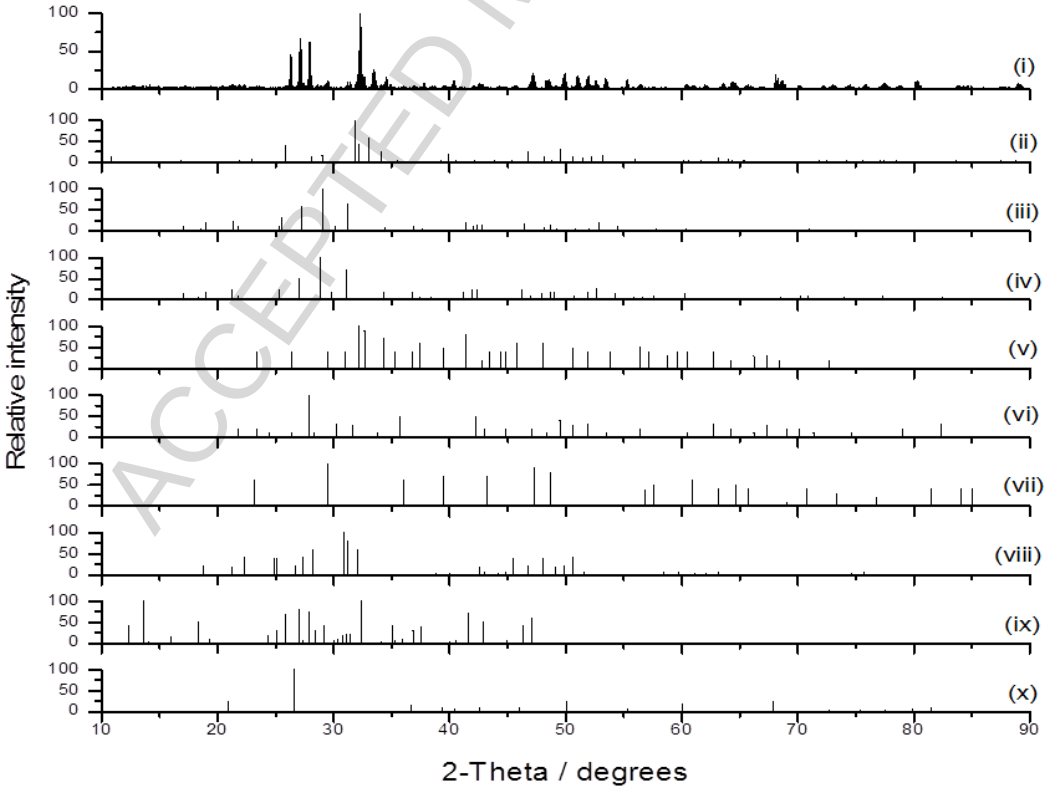

Figure 4. (a) XRD pattern of rare earth phosphate concentrate (REPC); (b) Comparison with standard patterns: (i) REPC, (ii) FAP (01-071-5050), (iii) cheralite (00-033-1095), (iv) monazite-Ce (00-011-0556), (v) calcium silicate (00-002-0843), (vi) calcium aluminium silicate (00-002-0523), (vii) calcite (00-002-0623), (viii) britholite-La (00-013-0106), (ix) kainosite-Y (00-014-0332) and (x) silicon dioxide (00-001-0649)

Fig. 5

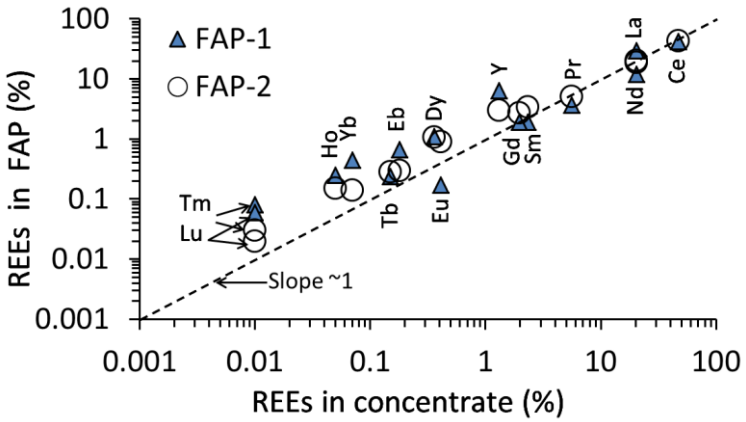

Figure 5. Correlation of REE composition in FAP and concentrate (data from Table 5)

Figure 6

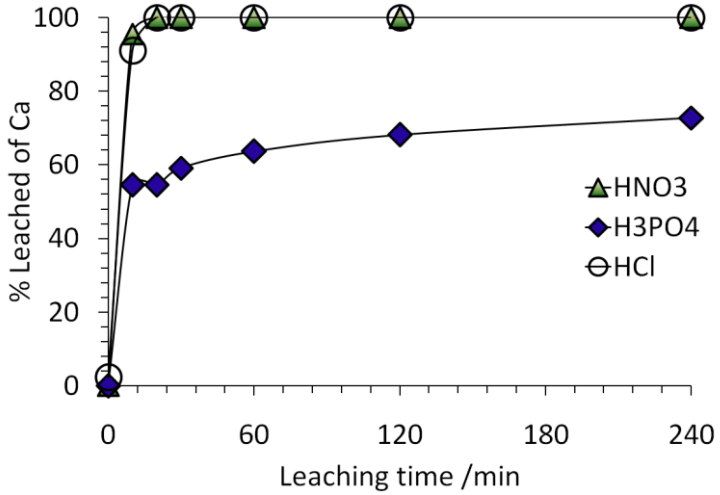

Figure 6. Calcium leach curve for fluorapatite (FAP-1) treated with different acids at leach conditions: acid concentrations of 3.25 M (HCl and HNO_3) and 2.28 M (H_3PO_4), 95 °C, 5% solids (w/w), agitation speed 1100 rpm.

Figure 7

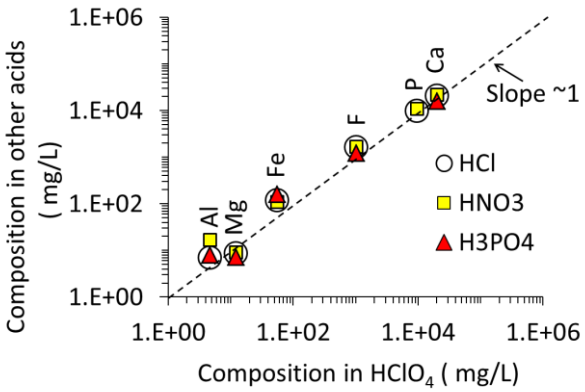

Figure 7. Composition of leach liquors form FAP1 in different acids after 4 h (data from Table 7)

Figure 8

(a)

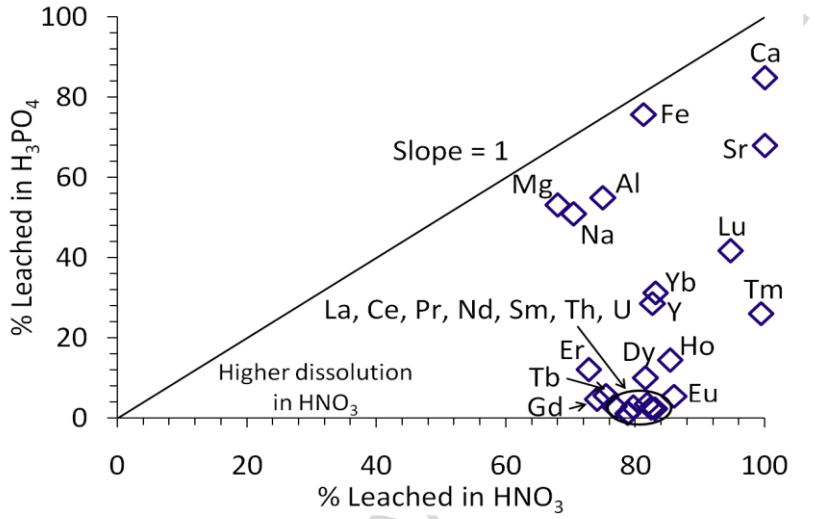

(b)

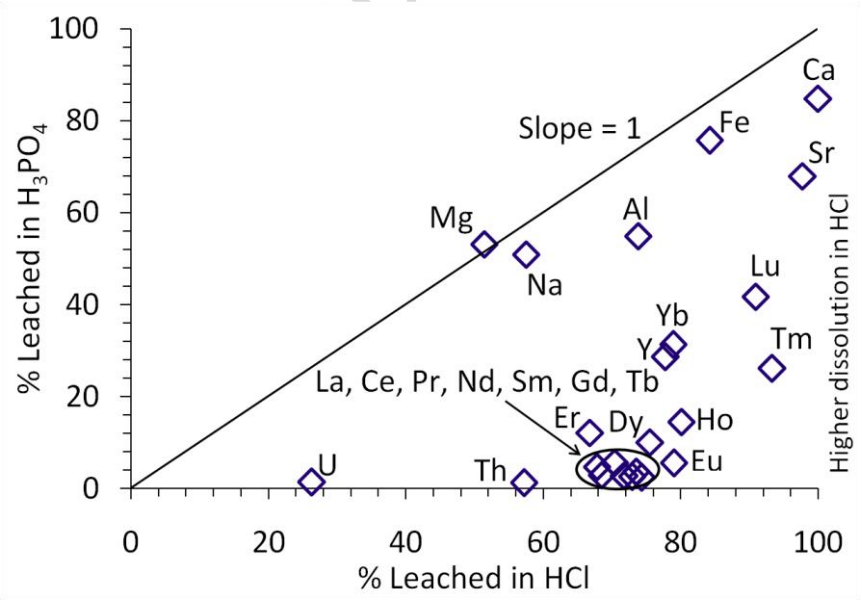

Figure 8. Comparison of metal ion leach efficiencies in HCl, HNO_3 and H_3PO_4 from concentrate at leach conditions: 3.25 M (HCl and HNO_3) and 2.28 M (H_3PO_4), 95 °C, 5% solids (w/w), agitation speed 1100 rpm, 4 h leach duration.

Figure 9

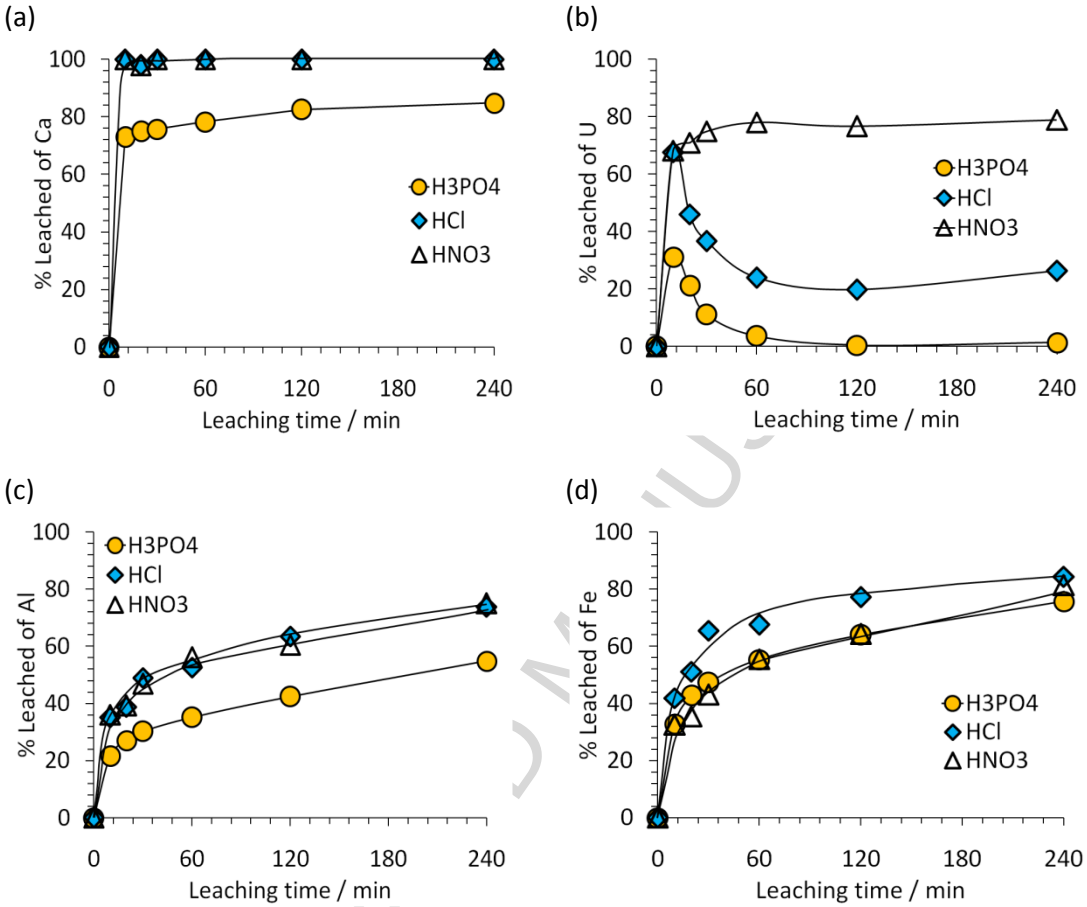

Figure 9. Selected metal ion leach curves of concentrate in different acids:
(a) calcium, (b) uranium, (c) aluminium and (d) iron at leach conditions same as in Fig. 8.

Figure 10

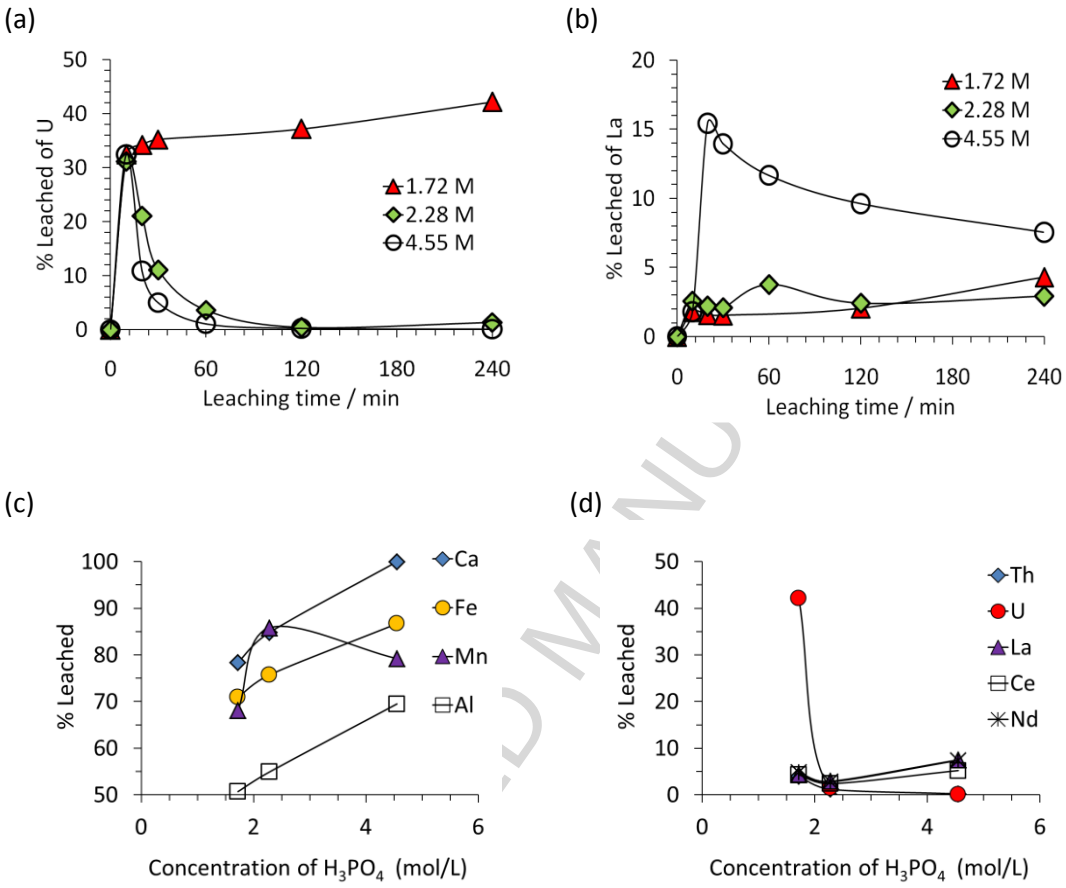

Figure 10. Effect of H_3PO_4 concentration on leaching efficiency of metal ions from concentrate (Table 10) at leach conditions: : 95 °C, 5% solids (w/w), agitation speed 1100 rpm, 4 h leach duration (Figures 10c and 10d).

Figure 11

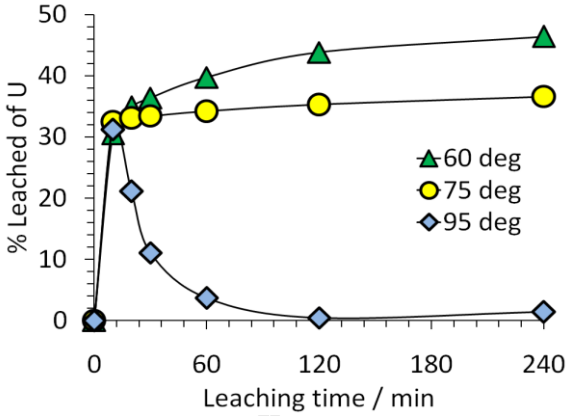

Figure 11. Effect of temperature on uranium leaching in H_3PO_4 at leach conditions: 2.28 M acid, 5% solids (w/w), agitation speed 1100 rpm, 4 h leach duration.

Figure 12

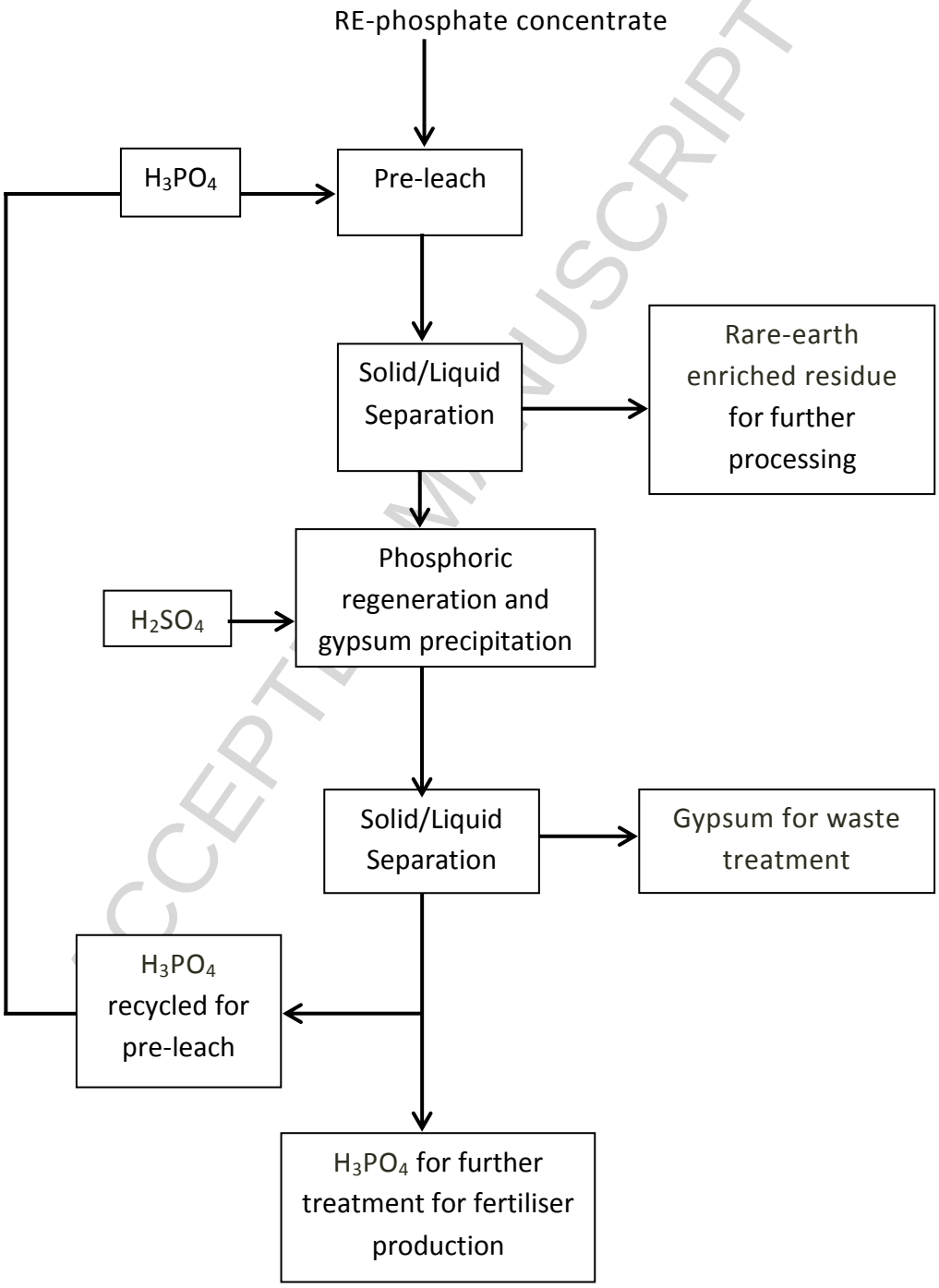

Figure 12. A simplified conceptual block diagram for phosphoric acid pre-leach

Table 1. Reactions of different acid pre-leach of fluorapatite

Reaction Number	Chemical Reaction	References
1	$Ca_{10}(PO_4)_6F_2 + 10H_2SO_4 = 6H_3PO_4 + 2HF + 10CaSO_4(s)$	Olanipekun, 1999; Wilemon, and Scheiner, 1987; Wang *et al.*, 2010
2	$Ca_{10}(PO_4)_6F_2 + 20HNO_3 = 6H_3PO_4 + 2HF + 10Ca(NO_3)_2$	Habashi, 1998; Li *et al.*, 2006; Jorjani *et al.*, 2011
3	$Ca_{10}(PO_4)_6F_2 + 20HCl$ (or $HClO_4$) $= 6H_3PO_4 + 2HF + 10CaCl_2$ (or $Ca(ClO_4)_2$)	Zafar *et al.*, 2006; Dorozhkin, 2012; Bandara and Senanayake, 2015
4a	$Ca_{10}(PO_4)_6F_2 + 14H_3PO_4 = 2HF + 10Ca(H_2PO_4)_2$	Zafar *et al.*, 2006; Habashi, 1998; Wang *et al.*, 2010; Antar and Jemal, 2008
4b	$Ca_{10}(PO_4)_6F_2 + 14H_3PO_4 = 2HF + 10Ca(H_2PO_4)^+ + 10H_2PO_4^-$	Brahim et al., 2008
4c	$10Ca(H_2PO_4)_2 + 10H_2SO_4 = 10CaSO_{4\,(s)} + 20H_3PO_4$	-

Table 2. Conditions for acid pre-leach used in previous studies

Acid	HNO_3	HCl
Pulp density (solids % (w/w))	38	28
Temperature	22-60 °C (uncontrolled)	21-44 °C (uncontrolled)
Acid Concentration	54% (w/w) (≈11 M)	20% (w/w)

(Mackowski et al., 2011)

Table 3. Test conditions in this work for pre-leach of concentrate

Acid Used	Temperature (°C)	Solids (% (w/w))	Acid Concentration (mol/L)
H_3PO_4	60	5	2.28
	75	5	2.28
	95	5	2.28
	95	5	1.72
	95	10	4.80
	95	15	7.63
	95	5	4.55
	95	5	2.28
	95	5	3.25
HCl	95	5	3.25
$HClO_4$	95	5	3.25
HNO_3	95	5	3.25

Table 4. Non-REE assays of fluorapatite and phosphate concentrate

Element	Mass percentages (%)		
	Concentrate	FAP-1	FAP-2
Ca	24.8	34.9	33.8
P	7.95	13.4	12.6
Na	0.13	0.25	0.19
Mg	0.49	0.01	0.01
Al	2.23	< 0.01	< 0.01
Si	9.05	0.22	0.09
S	0.10	0.09	< 0.01
F*	1.70	2.00	2.11
Fe	2.64	0.21	0.22
Sr	0.28	0.05	0.32
Th	0.48	0.03	0.01
U	0.03	<0.01	<0.01
Mn	0.02	-	-
Total REEs (lanthanides + Y)	4.91	1.25	0.55

* Based on XRF

Table 5. REE assays of fluorapatite and phosphate concentrate

Classification	Element	Mass percentages (%)		
		Concentrate	FAP-1	FAP-2
Light rare earths (LREs)	La	20.3	29.6	20.5
	Ce	47.0	41.6	43.4
	Pm	5.61	3.66	5.07
	Nd	20.3	11.9	19.0
Medium rare earths (MREs)	Sm	2.33	1.91	3.38
	Eu	0.41	0.17	0.90
	Gd	1.96	1.91	2.75
Heavy rare earths (HREs)	Y	1.31	6.38	3.01
	Tb	0.15	0.24	0.28
	Dy	0.36	1.10	1.06
	Ho	0.05	0.25	0.15
	Er	0.18	0.67	0.30
	Tm	0.01	0.08	0.03
	Yb	0.07	0.44	0.14
	Lu	0.01	0.06	0.02
Total REEs		100	100	100

Table 6. REE and non-REE assays of solid residues of phosphate concentrate

Element	Mass percentages (%) of solid residues in different acids								
	$HClO_4$ 3.25 M 95 °C	HNO_3 3.25 M 95 °C	HCl 3.25 M 95 °C	H_3PO_4					
				1.72 M 95 °C	2.28 M 95 °C	3.25 M 95 °C	4.55 M 95 °C	2.28 M 75 °C	2.28 M 60 °C
Ca	2.92	3.82	3.96	14.6	6.59	2.91	2.45	6.86	5.2
P	1.33	1.12	3.97	8.54	10.6	9.23	9.79	7.58	8.3
Na	0.16	0.19	0.21	0.14	0.1	0.1	0.08	0.14	0.15
Mg	0.42	0.57	0.67	0.48	0.21	0.28	0.22	0.55	0.43
Al	1.94	2.65	2.1	2.14	1.21	1.33	1.07	2.48	2.82
Si	19.7	23.2	23.4	11.5	10.5	11.6	10.3	14.4	14.5
Fe	1.36	2.08	1.19	1.89	0.67	1.04	0.75	2.33	2.83
Sr	0.08	0.1	0.07	0.18	0.1	0.12	0.1	0.16	0.13
Th	0.5	0.32	0.37	0.63	0.64	1.01	0.94	0.9	0.59
U	0.02	0.02	0.04	0.03	0.04	0.04	0.06	0.04	0.03
Total REEs (Ln + Y)	4.18	3.66	2.77	6.86	6.47	9.65	8.59	9.12	6.63

Leach conditions used: P_{80} = 165 µm, 5% solids (w/w), agitation: 1100 rpm, leach duration 4 h.

Table 7. Final leach liquor assays for fluorapatite dissolution in different acids

Elements	Elemental assays (mg/L) in different acid leach liquors of FAP-1[a]			
	3.25 M $HClO_4$[b]	3.25 M HCl	3.25 M HNO_3	2.28 M H_3PO_4
Ca	20000	21000	22000	16000
P	9500	10000[a]	11000[a]	21000
F	1024	1656	1705	1245
Al	4.6	7.00	17.0	8.00
Fe	55	120	110	160
Mg	12.2	8.80	9.20	7.20
Mn	-	6.50	6.90	5.70

a. ***Leach conditions used: P_{80} = 165 µm, 95 °C, 5% solids (w/w), agitation: 1100 rpm, leach duration 4 h.***

b. ***Data for FAP-2***

Table 8. Equilibrium constants for dissociation (K) or formation (β)

Reaction Number	Reaction	Log K or Log β (25°C)
5	$H_3PO_4 = H^+ + H_2PO_4^-$	-2.14[p]
6	$H_2PO_4^- = H^+ + HPO_4^{2-}$	-7.21[p]
7	$HPO_4^{2-} = H^+ + PO_4^{3-}$	-12.3[p]
8	$H_2PO_4^- = 2H^+ + PO_4^{3-}$	-19.6[q]
9	$H_3PO_4 = 3H^+ + PO_4^{3-}$	-21.7[q]
10	$Ca^{2+} + PO_4^{3-} + H^+ = CaHPO_4^0$	15.1[q]
11	$Ca^{2+} + HPO_4^{2-} = CaHPO_4^0$	2.80[p]
12	$Ca^{2+} + PO_4^{3-} + 2H^+ = Ca(H_2PO_4)^+$	21.0[q]
13	$Ca^{2+} + HPO_4^{2-} + H^+ = Ca(H_2PO_4)^+$	8.30[p]
14	$Al^{3+} + H_2PO_4^- = Al(H_2PO_4)^{2+}$	3.15[r]
15	$Al^{3+} + 2H_2PO_4^- = Al(H_2PO_4)_2^+$	5.54[r]
16	$Al^{3+} + HPO_4^{2-} = Al(HPO_4)^+$	8.81[r], 12.1[s]
17	$Al^{3+} + 2HPO_4^{2-} = Al(HPO_4)_2^-$	15.8[r]
18	$Fe^{3+} + H_2PO_4^- = Fe(H_2PO_4)^{2+}$	21.8[s]
19	$Fe^{3+} + HPO_4^{2-} = Fe(HPO_4)^+$	9.00[s]

Ionic strength 0-1 (data from [p]Senanayake et al., 2014a,b and references therein; [q] Zhang et al. (2012); [r]Savenko et al. (2005) ; [s]Sedlak (1991))

Table 9.The Ca/P molar ratios in final leach liquors in different acids

Feed material	Ca/P molar Ratio in solid	Experimental Ca/P molar Ratio in Leach Liquor			
		3.25 M $HClO_4$	3.25 M HCl	3.25 M HNO_3	2.28 M H_3PO_4
FAP-1	1.7[a]	1.6	1.6	1.5	0.6
Concentrate	2.4[b]	2.0	2.7	2.3	1.7

a. Based on theoretical formula
b. Based on actual assays (Table 7)

Table 10.Effect of acids on leaching efficiency of metal ions from concentrate

Acid Used	Temp:/ (°C)	Solids (%(w/w))	Acid Con: (mol/L)	Leached percentages (%)									
				Ca	P	F	Fe	Al	U	Th	La	Ce	Nd
H_3PO_4	60	5	2.28	98.6	-	-	30.9	26.9	46.4	0.89	3.02	2.16	2.75
	75	5	2.28	98.4	-	-	62.7	44.5	36.6	0.30	2.29	1.51	1.91
	95	5	2.28	84.8	-	30.2	75.7	54.9	1.37	1.24	2.93	2.41	2.80
	95	5	1.72	78.4	-	30.9	70.9	50.7	42.1	4.00	4.30	4.25	4.82
	95	10	4.80	99.3	-	-	82.0	64.4	0.18	0.33	4.31	3.01	3.80
	95	15	7.63	94.8	-	-	71.5	64.2	0.22	1.06	6.12	4.37	5.98
	95	5	4.55	100	-	39.0	86.7	69.5	0.10	0.20	7.50	5.20	7.40
	95	5	3.25	100	-	38.0	74.5	57.0	-	0.30	3.30	2.20	2.30
HCl	95	5	3.25	100	96.5	29.3	84.2	73.8	26.3	57.2	68.5	74.3	71.8
$HClO_4$	95	5	3.25	100	100	28.9	80.4	76.4	52.0	40.5	46.9	50.8	50.0
HNO_3	95	5	3.25	100	100	32.6	81.3	75	78.9	78.8	76.8	83.0	79.7

Agitation: 1100 rpm, 4 h leach duration (some of these leaching conditions were used for fluorapatite as well (leaching results of fluoraptite samples are in Table 7)

Table 11. Formation constants and solubility products for light rare earth phosphates.

Rare Earth Metal ion	Formation Constants		
	log β $M(H_2PO_4)^{2+}$	log β $M(HPO_4)^{+}$	-log K_{sp} (pK_{sp}) MPO_4 (solids)
La^{3+}	1.79	4.11	25.7 (26.2)*
Ce^{3+}	1.92	4.32	26.2
Pr^{3+}	2.00	4.45	26.4 (26.1)*
Nd^{3+}	2.05	4.54	26.2 (26.0)*

Formation constants correspond to the reaction of formation of these species from M^{3+} cation and $H_2PO_4^-$, HPO_4^{2-} or PO_4^{3-} anions; log β (25^0C, ionic strength = 0.1 mol kg^{-1}); log Ksp (25^0C, ionic strength = 0) from Liu and Byrne (1997); *Firsching and Brune (1991)

Table 12. Formation constants for fluoride complexes

Reaction Number	Reaction	Log β (25°C)
20 [a]	$H^+ + F^- = HF^0$ (I = 1)	2.98
21 [a]	$HF + F^- = HF_2^-$ (I = 1)	0.73
22 [a]	$Ca^{2+} + F^- = CaF^+$ (I=1)	0.53
23 [a]	$Mg^{2+} + F^- = MgF^+$ (I=1)	1.38
24 [b]	$Al^{3+} + F^- = AlF^{2+}$ (I = 0.5)	6.13
25 [b]	$Al^{3+} + 2F^- = AlF_2^+$ (I = 0.5)	11.2
26 [b]	$Al^{3+} + 3F^- = AlF_3^0$ (I = 0.5)	15.0
27 [b]	$Al^{3+} + 4F^- = AlF_4^-$ (I = 0.5)	17.7
28 [b]	$Al^{3+} + 5F^- = AlF_5^{2-}$ (I = 0.5)	19.4
29 [a]	$Al^{3+} + 6F^- = AlF_6^{3-}$ (I = 0.5)	19.8
30 [a]	$Fe^{3+} + F^- = FeF^{2+}$ (I = 1)	5.19
31 [a]	$Fe^{3+} + 2F^- = FeF_2^+$ (I = 1)	9.12
32 [a]	$Fe^{3+} + 3F^- = FeF_3^0$ (I = 1)	12.1
33 [a]	$UO_2^{2+} + F^- = UO_2F^+$ (I=1)	4.54
34 [a]	$UO_2^{2+} + 2F^- = UO_2F_2^0$ (I=1)	7.98
35 [a]	$UO_2^{2+} + 3F^- = UO_2F_3^-$ (I=1)	10.4
36 [a]	$UO_2^{2+} + 4F^- = UO_2F_4^{2-}$ (I=1)	11.9
37 [a,c]	$Th^{4+} + F^- = ThF^{3+}$ (I = 1)[a]	8.08[a], 7.51[c]
38 [a]	$ThF^{3+} + F^- = ThF_2^{2+}$ (I = 1)	6.36
39 [a]	$ThF_2^{2+} + F^- = ThF_3^+$ (I = 1)	4.57
40 [a]	$ThF_3^+ + F^- = ThF_4^0$ (I = 1)	3.28
41 [c]	$Th^{4+} + 2F^- = ThF_2^{2+}$	13.3
42 [c]	$Th^{4+} + 3F^- = ThF_3^+$	8.58
43 [c]	$Th^{4+} + 4F^- = ThF_4^0$	20.2

I = Ionic strength

[a] Högfeldt, 1982

[b] Hem, 1968

[c] HSC 7.1 database

Table 13. Formation constants for precipitation and dissociation of phosphates

Reaction Number	Reaction	pK_{sp} at 25^0C
44[a]	$Al^{3+} + PO_4^{3-} = AlPO_4(s)$	20.0
45[a]	$Fe^{3+} + PO_4^{3-} + 2H_2O = FePO_4.2H_2O(s)$	15.0
46[b]	$AlPO_4(s) + 2H^+ = AlH_2PO_4^{2+}$	2.75
47[b]	$AlPO_4(s) + 4HF^0 = AlF_4^- + 2H^+ + H_2PO_4^-$	5.38
48[b]	$FePO_4.2H_2O(s) + 2H^+ = FeH_2PO_4^{2+} + 2H_2O$	26.4
49[b]	$FePO_4.2H_2O(s) + 3HF^0 = FeF_3^0 + H^+ + H_2PO_4^- + 2H_2O$	7.76
50[c,d]	$Ca^{2+} + 2UO_2^{2+} + 2PO_4^{3-} + 3H_2O = Ca(UO_2)_2(PO_4)_2.3H_2O(s)$	48.4
51[c,e]	$UO_2^{2+} + HPO_4^{2-} + 3H_2O = UO_2HPO_4.3H_2O(s)$	13.2
52[c,f]	$3UO_2^{2+} + 2PO_4^{3-} + 4H_2O = (UO_2)_3(PO_4)_2.4H_2O(s)$	49.4

[a] Haynes et al. (2014-2015)
[b] Calculated using reactions in tables
[c] Gorman-Lewis et al. (2009)
[d] Autunite: $Ca(UO_2)_2(PO_4)_2$
[e] Uranyl hydrogen phosphate: $UO_2HPO_4.3H_2O$
[f] Uranyl orthophosphate: $(UO_2)_3(PO_4)_2.4H_2O$

Table 14. Solubility products of rare earth phosphate at different temperatures.

Element	log K_{sp} at different temperatures				
	Liu and Byrne (1997)	Firsching and Brune (1991)		Ziya et al, (2005)	
	25 °C[a]	25 °C	72 °C	23 °C	50 °C
La	-25.7	-26.2	-26.5	-24.7	-25.4
Ce	-26.2	-	-		
Pr	-26.4	-26.1	-26.5		
Nd	-26.2	-26.0	-25.5	-25.8	-26.6
Sm	-26.1	-26.0	-26.6	-24.6	-24.8
Eu	-25.9	-25.8	-26.4		
Gd	-25.6	-25.4	-25.8		
Tb	-25.3	-25.1	-26.0		
Dy	-25.1	-25.2	-25.7		
Ho	-25.0	-25.6	-		
Er	-25.1	-25.8	-25.9		
Tm	-25.0	-26.1	-26.2		
Yb	-24.8	-26.2	-26.3		
Lu	-24.7	-25.4	-26.0		
Y	-25.0	-24.8	-	-27.9	-27.8

Highlights

- High leaching of calcium and phosphorus in $HClO_4$, HCl and HNO_3, but low leaching in H_3PO_4.
- Results consistent with the formation of phosphate/fluoride complex species in solution.
- Low leaching of RE/uranyl/thorium ions in H_3PO_4 due to the formation of phosphate precipitates.
- Selective leaching of calcium and some other metals leaving uranium, thorium and REEs in the residue suitable for acid bake